DASA-13.018

Technical Report **R 536**

STATIC AND DYNAMIC BEARING TESTS ON A STRIP FOOTING IN SATURATED SAND

June 1967

NAVAL FACILITIES ENGINEERING COMMAND

NAVAL CIVIL ENGINEERING LABORATORY

Port Hueneme, California

STATIC AND DYNAMIC BEARING TESTS ON A STRIP FOOTING IN SATURATED SAND

Technical Report R-536

Y-F008-08-03-402, DASA-13.018

by

Charles R. White

ABSTRACT

This report describes the static and dynamic loading of a 12-inch-wide by 18-inch-deep by 6-foot-long rigid footing, representing the strip footing of a subsurface shelter. Boundary conditions simulated those of a torsionally restrained footing of a flexible arch structure with simulated overburden of 20 feet at one side of the footing. Saturated and partially saturated sand was the test soil. Several soil void ratios were employed, and the effect on the relationship between load and displacement of the footing caused by soil saturation at void ratios higher than the critical void ratio was demonstrated.

Distribution of this report is unlimited.

Copies available at the Clearinghouse for Federal Scientific & Technical Information (CFSTI), Sills Building, 5285 Port Royal Road, Springfield, Va. 22151
Price $3.00

The Laboratory invites comment on this report, particularly on the results obtained by those who have applied the information.

This work sponsored by the Defense Atomic Support Agency.

CONTENTS

	page
INTRODUCTION	1
STATEMENT OF PROBLEM	1
SCOPE AND APPROACH	2
TEST DESCRIPTION	3
Test Method and Apparatus	3
Soil Properties and Preparation	8
Instrumentation	11
Test Schedule	12
RESULTS AND DISCUSSION	13
CONCLUSIONS	23
FUTURE PLANS	24
ACKNOWLEDGMENTS	24
REFERENCES	25

INTRODUCTION

This fourth report in a series on soil bearing capacity experiments at the Naval Civil Engineering Laboratory (NCEL) is the first to consider saturated soil. The other series of tests were made in dry sand. The first report covered the results of tests of statically and dynamically loaded spread footings on the soil surface.[1] The second report concerned static and dynamic loading of a spread footing at several different simulated depths of burial.[2] The third test series[3] featured the first change from the 15-inch-diameter plate of the first two programs and involved a 12-inch-wide strip footing loaded dynamically while under various amounts of simulated overburden maintained at one side of the footing. The fourth test series, which is reported here, also concerned a strip or wall footing, but under simulated overburden of a single magnitude (15 psi) applied at one side. The saturated soil condition of the fourth series is more representative of many sites of Navy shore facilities than the dry condition tested in the earlier series. The work was performed under Work Unit Y-F008-08-03-402 (DASA-13.018), "Fundamental Behavior of Soils Under Time-Dependent Loads," sponsored by the Defense Atomic Support Agency through the Naval Facilities Engineering Command.

STATEMENT OF PROBLEM

One of the major problem areas in soil dynamics continues to be the lack of sufficient practical information for the design of footings for structures to be loaded dynamically. This is particularly true of buried structures. In this complex situation, the load is carried through the soil to the structure and partly returned to the soil by the footings. The weight of static overburden influences the load-carrying capacity of soil beneath the footing and hence influences the load-versus-displacement characteristics of the footing. Surface blast overpressure, acting somewhat as increased overburden, also may have some significant effect upon the behavior of the footing. Additionally, the response of dynamically loaded soils is modified by the presence of pore water in various degrees of soil saturation.

A better understanding is needed of the interrelationships of the various natural and man-imposed soil conditions which affect the load-displacement behavior of footings. This information is especially needed for designing the footings of flexible, arch-shaped structures. Such structures depend upon active soil arching and passive

soil pressure for part of their structural integrity. The mobilization of these soil pressures is, in turn, influenced by the deformation and the displacement of the structure. Prediction and control of the displacement of the structure is possible through proper selection of footing size. Such footing size selection will be easier and more accurate when a more complete body of load-versus-displacement information is available from dynamic tests of footings. The continuing ban on nuclear air blasts precludes field testing to fill this information gap. Field testing with chemical explosives places size limitations upon the test elements. Laboratory testing, for the most part, has been limited to rather small-sized structures and footings. Extrapolation of results of these tests of small-sized structures and footings to predictions of full-scale behavior generally is difficult and sometimes is of dubious accuracy. Some recent notable successes have been achieved in extrapolating results of small-scale tests in cohesive soils.[4] However, those tests did not include the effects of overburden.

To reiterate, large-scale tests are needed of dynamically loaded footings in various types of soil with overburden. The empirical information thus gained is required for development or modification of theoretical methods for treating structural design problems. Definition of the effect of pseudo-overburden produced by surface blast pressure also is needed.

SCOPE AND APPROACH

The tests reported here were made on 6-foot lengths of full-sized strip footing loaded statically and dynamically in saturated sand. The cross section of the footing, 12 inches wide by 18 inches deep, was the same as the footings of Structure 3.3b, which was subjected to the effects of a nuclear blast during Operation PLUMBBOB.[5] Depth of overburden above the footing during the field test was 19 feet. The simulated depth in the laboratory experiment was approximately 20 feet.

During the field testing of PLUMBBOB Structure 3.3b, the footings experienced some torsional distress. Consequently, any future installation of this type of structure should incorporate facilities to prevent rotation of the footings about a longitudinal axis. Therefore, antirotation features were incorporated in the laboratory experiments reported here.

The PLUMBBOB experiments were made at the Nevada Test Site of the Atomic Energy Commission during the dry season of the year. Hence, ground water was not a factor in the tests. However, information is needed about the influence of saturation on the behavior of dynamically loaded footings. Accordingly, the NCEL experiments reported here were made in saturated sand.

Ultimately, the effect of pseudo-overburden caused by surface blast pressure should be investigated. However, investigation of that aspect of the load-versus-displacement phenomenon of footings was not within the scope of the tests reported here. These tests were a simulation of the environment of a wall footing of a structure buried in sand and subjected to dynamic loads. For most of the tests, the water table was at the bottom of the footing. For a few tests, the water table was depressed below that elevation.

TEST DESCRIPTION

Test Method and Apparatus

The experiments consisted of vertically loading a footing along its top surface while maintaining an overburden along one side and a water table at the bottom elevation of the footing.

Dynamic loads on the footings were produced by the NCEL atomic blast simulator.[6] The pressures of an explosion confined in the blast simulator were made to impinge upon a horizontal steel beam placed between the parallel, downward-projecting skirts of the simulator. The load thus collected by the beam was transmitted down through three short steel columns. The load in each column passed through a load-measuring cell to a steel load distributor mounted on the top of the footing. The footing was supported on sand in the 9-foot by 10-foot concrete-walled pit beneath the simulator. Depth of sand in the concrete-walled pit was 10-1/2 feet. The test footing was 12 inches wide, 18 inches deep, and 6 feet long.

In the prototype structure upon which the design of this experiment was partly based, the load was applied by the structure to the footing essentially as a line load along the spring line of the structure. Certain features of the overburden simulation apparatus of the experiment, which will be described later, prevented application of a continuous line load to the experimental footing. Instead, the load was applied through load distributors along three equal lengths of the footing. Load application was interrupted for 9-inch distances at the one-third points of the footing. Great care was taken to seat the load distributors on a lead sheet placed on the top of the footing so that stress concentrations would be avoided. However, in an earlier test series[3] some cracking of the concrete footing occurred. Therefore, for the experiments reported upon here, a footing having approximately the same mass but made of steel was used. The steel footing was fabricated using as a core a 5-foot 10-1/2-inch length of 18WF114 rolled steel beam. Steel plates of 3/4-inch thickness were welded to the ends and from flange to flange. The resulting steel box, with the web of the 18WF114 beam oriented vertically, weighed 1,205 pounds compared to 1,350 pounds for the concrete footing used previously. As with the formerly used concrete footing, the outside dimensions of the steel footing were 12 inches wide, 18 inches deep, and 6 feet long. Since the load distributors and the lead sheet were bolted to the steel footing, they must be considered part of the mass of the footing. Combined weight of the three load distributors and bolts was 315 pounds. The lead sheet weighed 46 pounds. Thus, the combined weight of the load distributors and bolts, the lead sheet, and the footing, was 1,566 pounds.

The combined weight of the loading beam and columns and of the load cells, all of which acted as a unit, was 1,151 pounds. Figure 1 shows comparative sketches of the field event and the laboratory simulation.

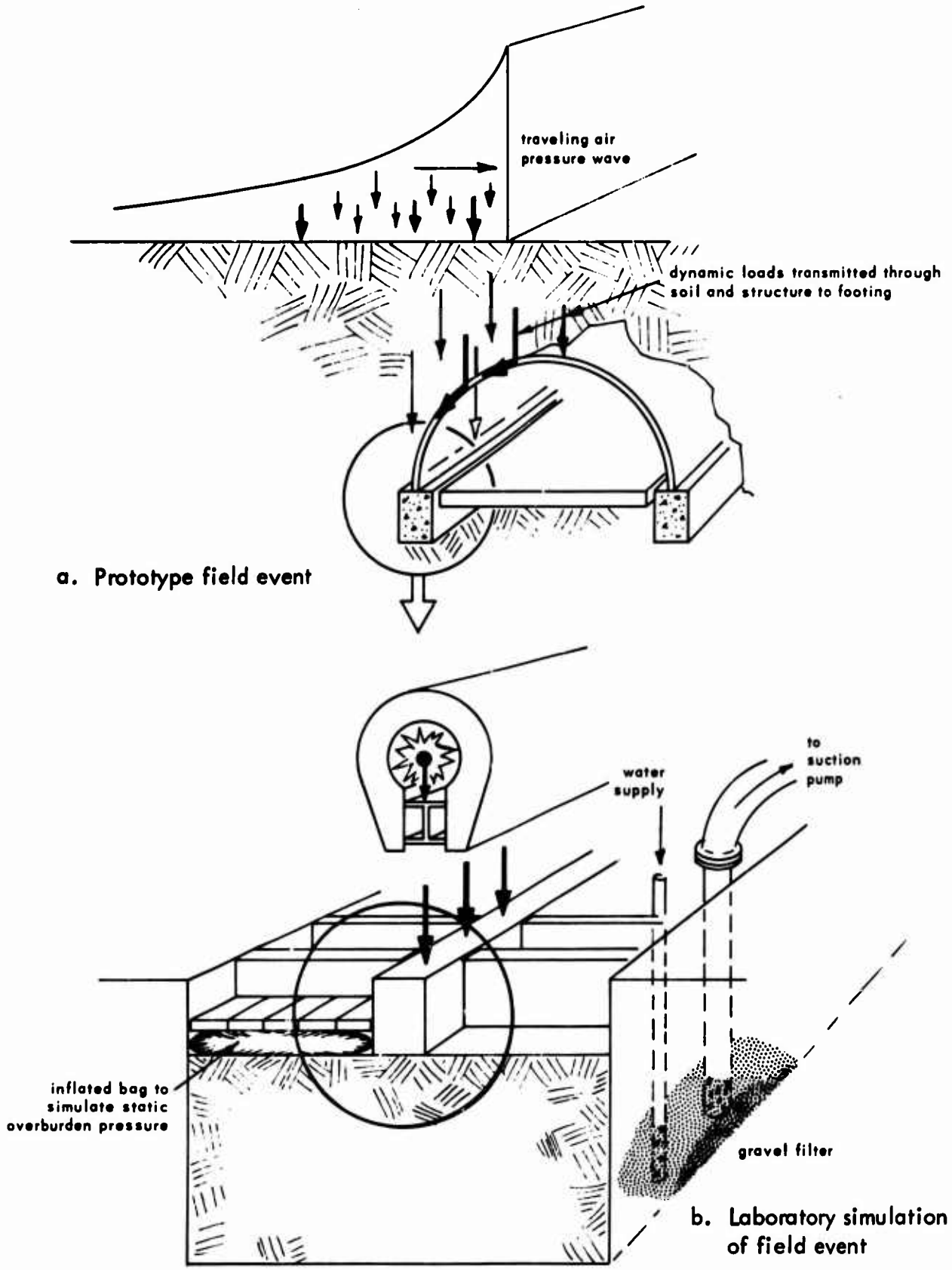

Figure 1. Prototype field event and laboratory simulation.

The soil placement and saturation will be described later. After the soil was prepared and the upper surface leveled, the test footing was placed on the soil directly beneath the blast simulator. One of the environmental conditions for these experiments was the maintenance of a static overburden on the soil on one side of the footing. There was insufficient room to place dead weight on the soil to provide this load. Instead, simulated overburden was provided by pressured gas in a flexible bag confined between the soil surface and a wooden deck 2 inches above the soil surface. For safety, dry nitrogen was used and pressurized to 15 psi. This is equivalent to a depth of approximately 20 feet of the soil used for the tests.

Details of the overburden-pressure apparatus were similar to those reported for spread-footing tests under overburden.[2] Briefly, vertical reaction for the wooden deck which restrained the pressurized bag was provided by vertical steel tie-rods which connected the ends of steel beams across the top of the pit with the ends of steel beams fastened to another wooden deck, or floor, beneath the soil. The pneumatic bag was wrapped in canvas for protection and was further protected by a Teflon rub-sheet at the surface of contact with the footing. The Teflon sheet reduced friction between the footing and the overburden apparatus. Figures 2 through 6 show the steps taken to prepare for a loading of the footing.

Another environmental condition for the footing was the provision of torsional restraint about the longitudinal axis of the footing. Horizontal ties between opposite footings of a structure probably will be used in actual field installations. However, this laboratory experiment only involved one footing, and the tied arrangement was not feasible. Instead, pairs of horizontal wooden beams were placed transversely in the test pit on opposite sides of the footing near the ends and at the one-third points to prevent rotation of the footing about its major horizontal axis. The outer ends of the beams were jacked against the walls of the pit. The inner ends of the beams were fitted with ground steel plates. The beams were jacked into position with sufficient clearance between the beam end-plates and the footing for two sheets of 0.010-inch Teflon film. Thus, the footing was only permitted to slide down without rotating during loading. The function of these antirotation beams is illustrated in Figure 5.

To best duplicate the field condition, a line load should have been applied to the top of the footing. The hold-down beams of the overburden apparatus necessarily had to span the test pit at two places above the footing. Therefore, the footing could not be loaded continuously along its top centerline. As mentioned earlier, steel load distributors were bolted to the top of the footing to provide as uniform a distribution of load as possible on the top of the footing. The spaces between the load distributors and the overburden hold-down beams which passed through those spaces may be seen clearly in Figures 5 and 6, respectively.

Figure 2. Test pit filled with compacted damp sand and footing in place.

Figure 3. Inflatable bag wrapped in canvas with Teflon rub-sheet in place between footing and bag.

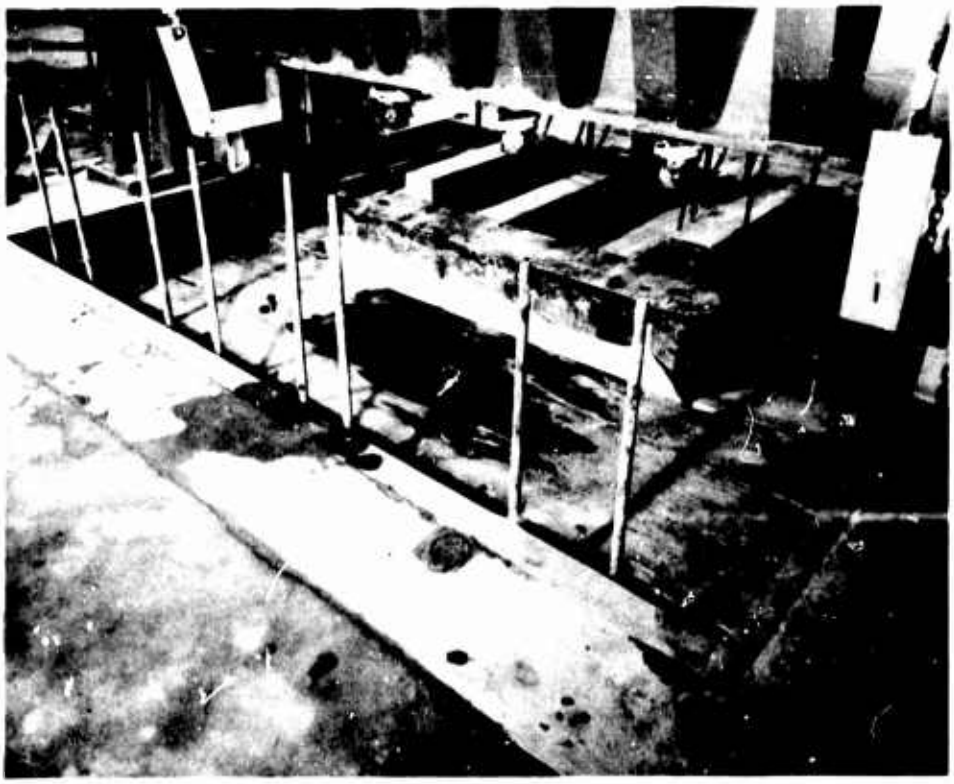

Figure 4. Upper horizontal deck in place.

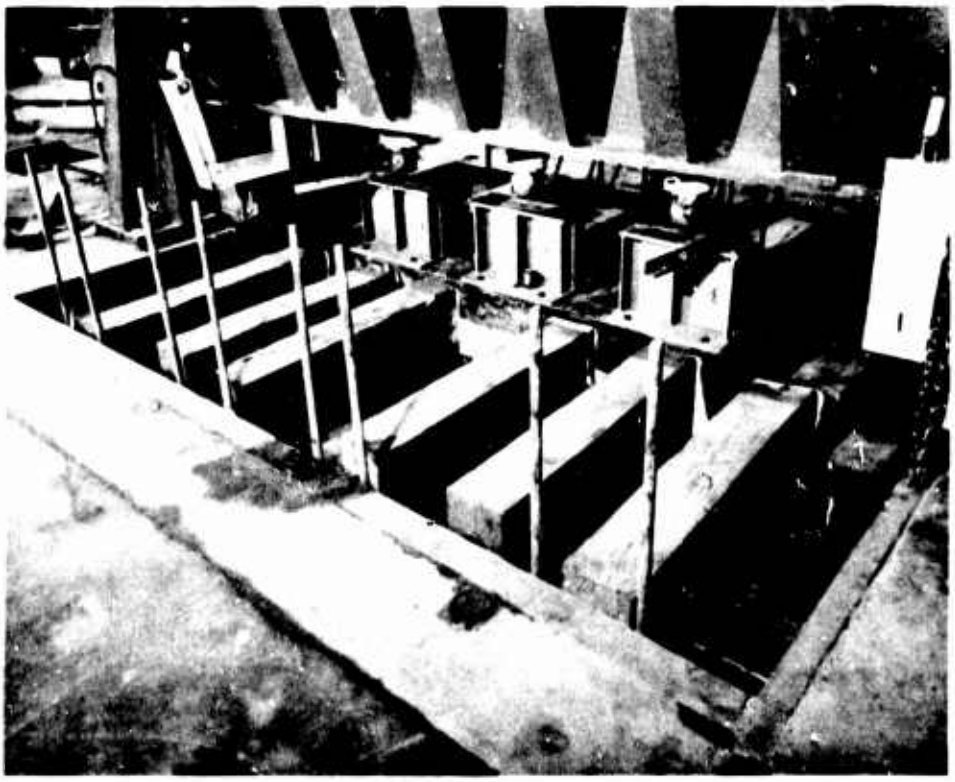

Figure 5. Footing antirotation beams in place and load spreaders mounted on footing.

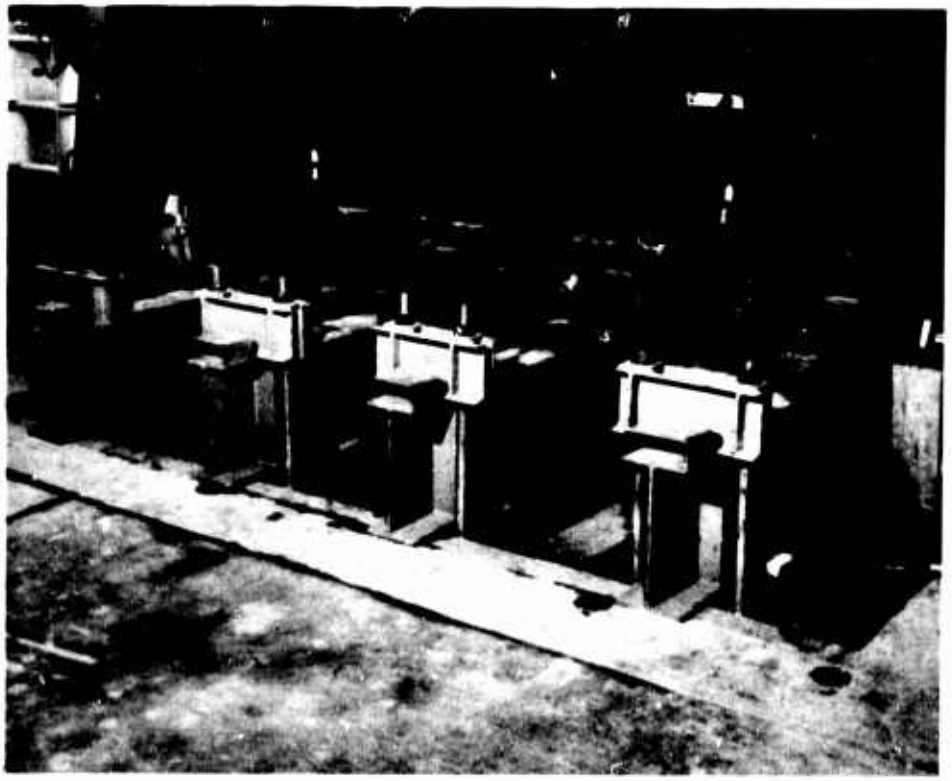

Figure 6. Steel reaction beams, tie-rod saddles, and potentiometers in place.

A third environmental factor, and the one which made these tests unique when compared with others of the series,[1,2,3] was the presence of pore water in the soil. This water was introduced at the bottom of the pit and allowed to rise through the voids, thereby preventing entrapment of air which would have occurred if water had been added from the top. Water was added through a 3-inch-diameter steel pipe near the centerline of the pit wall on the side not covered by the overburden apparatus. The lower end of the pipe was perforated and terminated in a half cubic yard of gravel banked about the pipe at the bottom of the pit. Also terminating in the gravel was a 6-inch-diameter suction pipe extending down from the surface adjacent and parallel to the supply pipe. The suction pipe was used for drawing down the water table in the pit to permit reprocessing soil in the upper zone. The supply and suction pipes can be seen in Figure 7.

Soil Properties and Preparation

The soil used for these experiments was taken from a river bed and screened to the gradation shown in Figure 8. It is primarily used locally as plasterer's sand, but large quantities of it have been used at NCEL for experimental studies of soil dynamics and studies of static and dynamic soil-structure interaction. Physical properties of the sand are shown in Table 1.

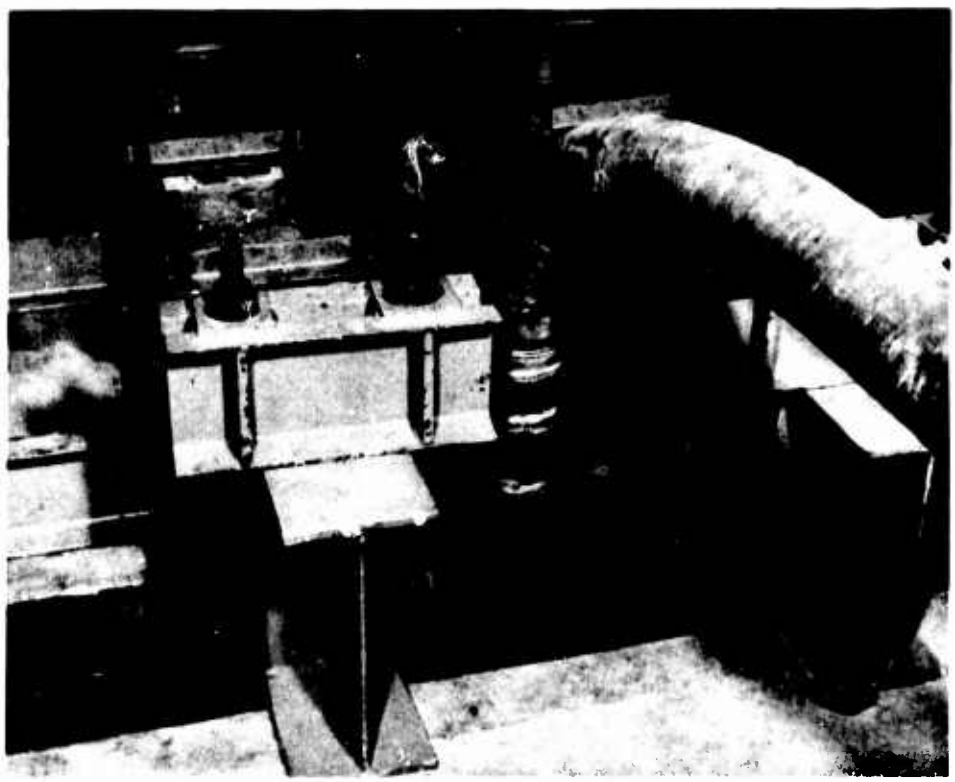

Figure 7. Supply and suction pipes for controlling water level in sand.

Table 1. Fundamental Physical Properties of Soil Used for Footing Tests

Type of soil	sand
Secant modulus of compression (consolidometer) at 50 psi:	
at density = 105.8 lb/ft^3 (psi)	6,500
at density = 111.9 lb/ft^3 (psi)	10,100
Cohesion (psi)	0
Static angle of internal friction at density = 112 lb/ft^3 (deg)	44
Dynamic angle of internal friction at density = 112.3 lb/ft^3 (deg)	43.1
Specific gravity	2.62
Maximum grain size (mm)	2.5
Effective size, D_{10} (mm)	0.21
Uniformity coefficient	3
Permeability	
at density = 95 lb/ft^3 (in./sec)	0.0116
at density = 105 lb/ft^3 (in./sec)	0.0096

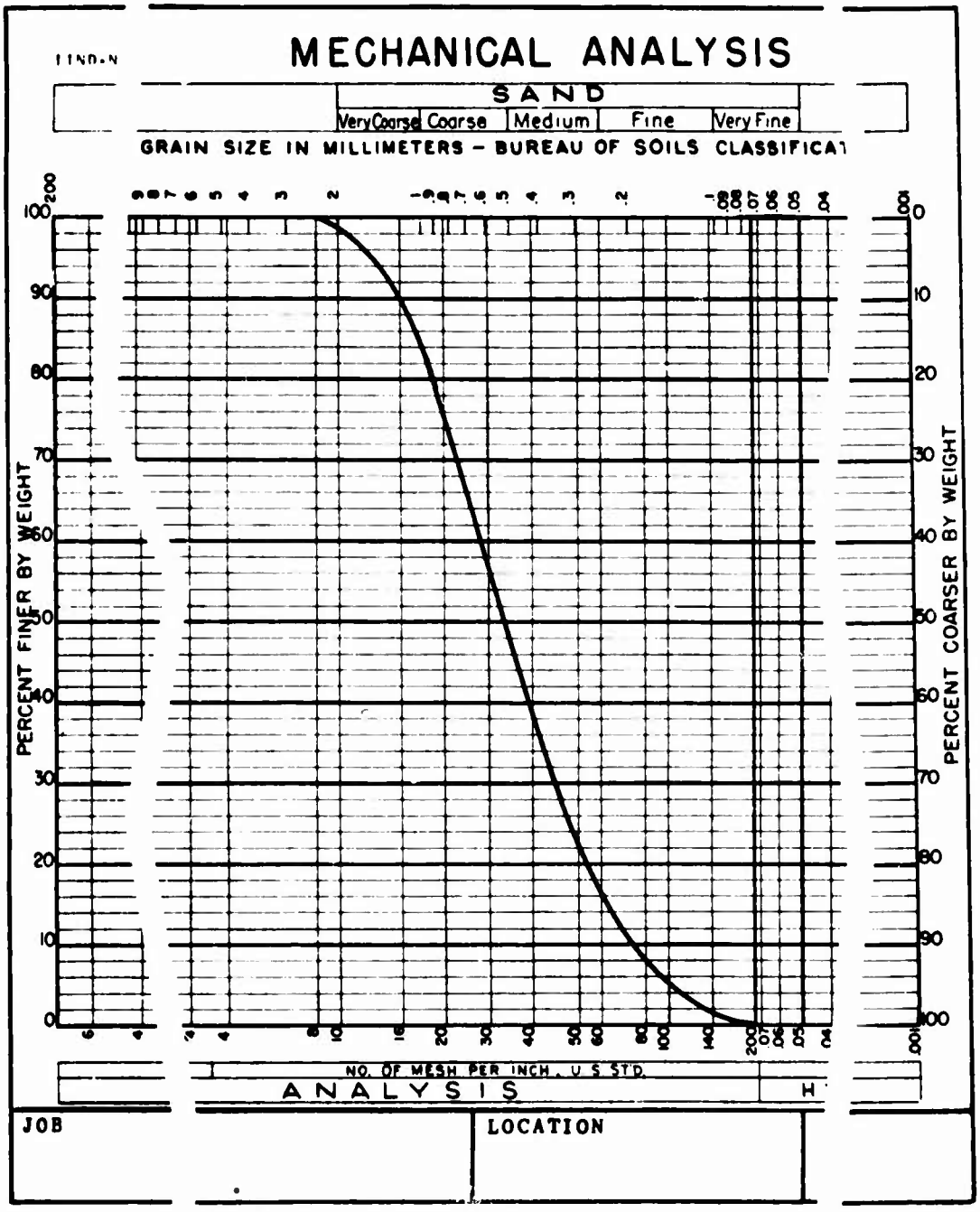

Figure 8. Grain size distribution of sand used for strip-footing tests.

The sand was placed in a damp condition (5 to 8% moisture) and spread in 2-foot layers. It was compacted by a Wacker Model EVR-120 electrically powered soil tamper. The tamper was moved about the surface of the layer being compacted in a regular pattern throughout the filling of the test pit. In-place density of the sand in each layer was measured by the method described in ASTM Designation D-1556-58T, "Density of Soil In-Place by the Sand-Cone Method." The average of 38 measured densities (converted to dry density) of sand in the test pit preceding the first loading of the footing was 109.8 lb/ft^3. This is a relative density of 78.6% based upon maximum and minimum densities of 114.7 lb/ft^3 and 95.0 lb/ft^3, respectively, for this sand.[7]

Following each loading of the test footing, the sand in the upper 20 inches of the test pit within a zone extending 12 inches on each side of the centerline of the footing was loosened by hand shoveling and reworked. The retamping was accomplished, as before, with the Wacker tamper. Attempts were made to recompact this zone of soil to one of two densities, which may be described generally as "loose" and "dense." Later comparison of results of the footing tests will be made upon the basis of these various initial conditions of the soil. To determine the void ratio of the reworked soil, in-place density of the soil was measured as before. Great care was taken in the compaction procedure to assure uniform density conditions throughout the reworked zone.

Instrumentation

With one exception, all instrumentation was standard, commercially available apparatus. All loads, pressures, and displacements were recorded using appropriate transducers in conjunction with carrier amplifiers and a recording oscillograph. The type 1-113B amplifiers and type 5-119 oscillograph used are designated "System D" by the manufacturer, Consolidated Electrodynamics Corporation, Pasadena, California.

Loads applied to the load-spreading devices on the top of the footing were measured by three 100-kip Baldwin type C compression load cells. Prior to the test program, the load cells were calibrated under static load in a hydraulically powered testing machine.

Statham model PA208TC pressure gages were used to measure pressures in the blast simulator and to monitor pressure in the inflated bag used to simulate overburden pressure. Prior to use, these gages and the pore pressure gage described below were calibrated against a precision dial pressure gage.

Vertical displacement of the footing was measured with two Bourns model 108 linear-motion potentiometers, which have 10 inches of travel. These instruments have a full stroke resistance of 10,000 ohms. The only nonstandard item of instrumentation was a supplementary bridge circuit used with each of these potentiometers to make them compatible with the System D equipment, which is designed for use with 120-ohm bridges. The supplementary circuit is shown schematically in Figure 9.

Pore pressure in the soil at a point 8-1/2 feet below the center of the test footing was monitored by a type 4-112 pressure gage manufactured by Consolidated Electrodynamics Corporation. The pressure-sensitive face of the gage was covered by a 200-mesh-per-inch wire screen so arranged that intergranular soil stresses were isolated from the gage but pore pressures were registered. A second pore pressure gage was installed at a depth of 4-1/2 feet below the center of the footing, but a failure occurred in the waterproofing material applied to the connector and no measurements were made with this gage.

Acceleration was measured by a Statham model A5-200-350 accelerometer bolted to the top of the footing. Before use, the accelerometer was calibrated in a centrifuge.

Test Schedule

The experimental program was designed to provide load-displacement data for sand loaded dynamically in each of two moisture conditions — drained and saturated. Within each moisture content group, two void ratio conditions were used — relatively high and relatively low. For each moisture condition and for each void ratio grouping, at least three different loads (low, medium, and high) were applied.

More specifically, the two groups of void ratios were planned to provide loose and dense soil conditions that it was hoped would bracket the critical void ratio. The void ratios utilized were the highest and lowest void ratios that could be achieved in the test sand with the equipment available. The loads selected for application

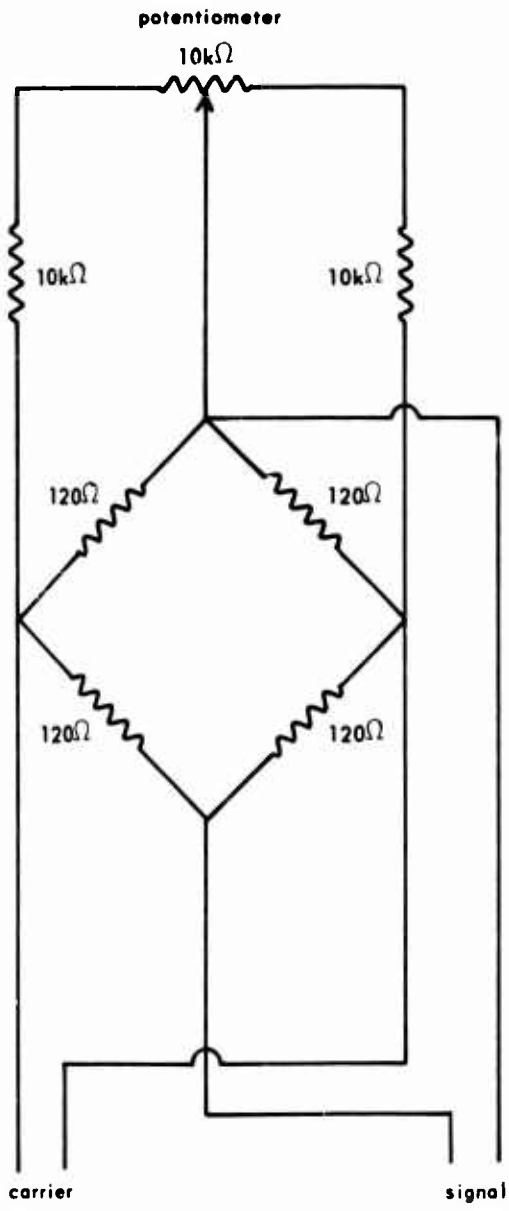

Figure 9. Schematic diagram of potentiometer and supplementary bridge circuit used to monitor footing displacement.

to the footings were chosen to provide a broad range of load values for the load-displacement graphs subsequently to be drawn. The three load ranges were low (i.e., up to 20 kips/ft^2 on the footing), medium (between 20 and 30 kips/ft^2), and high (above 30 kips/ft^2). The highest load was dictated by the capability of the blast simulator which permitted a maximum load of approximately 39 kips/ft^2 on the footings used for these tests.

In all tests having the water table at the elevation of the bottom of the footing, the water was brought to that level 15 minutes before applying overburden pressure. The overburden pressure was applied and maintained for 15 minutes prior to application of dynamic load to the footing. The overburden pressure was released immediately after the dynamic load decayed to zero.

RESULTS AND DISCUSSION

Table 2 lists the pertinent variables and measured results of these tests. Among the items shown are degree of saturation, initial void ratio, peak load and load duration, footing acceleration, displacement and associated time factors, and pore pressure information. Table 3 shows the results of the single static test.

The magnitude of the pore pressure at a point 8-1/2 feet below the center of the footing is not significant for the type of test reported. In an actual field situation, the air-blast-induced soil stresses would be propagated from a stress front covering a large horizontal surface area of the soil. Under field conditions, such pore pressures could conceivably have some effect upon the behavior of footings. The pore pressures generated in this experiment were caused only by penetration of the footing into the soil. The fact that excess pore pressure was developed (i.e., pore pressure greater than that at the ambient static equilibrium condition) and not the magnitude of that excess was the significant information sought in this initial NCEL dynamic experiment in saturated soil. Magnitude of the excess pore pressure at a depth 8-1/2 feet below the footing, and arrival time of the pore pressure wave, are shown in Table 2. For this and all other chronologically described events in the experiments, "zero time" was taken as the arrival time of the dynamic load on the top of the footing as indicated by initial excitation of the accelerometer mounted there.

As stated earlier, attempts were made to compact the soil in the zone surrounding the footing to two different initial densities. It is very difficult to select a desired density and actually achieve that magnitude with any great precision. However, the density of the soil surrounding the footing for any given test is considered to have been uniformly achieved for that test. The various tests were grouped on the basis of similar initial void ratio of the soil. Maximum footing loads on the soil versus corresponding maximum vertical displacements of the footing within each void ratio grouping, moisture condition, and type of load were subjected to a computer-processed regression analysis. Load was selected as the independent variable. Results of these regression analyses are shown individually for each group in Figures 10 through 15. A composite of these graphs is shown in Figure 16 to facilitate the discussion which follows.

Table 2. Results of Dynamic Tests on a Strip Footing Buried in Saturated Sand

Test No.	Degree of Saturation (%)	Initial Void Ratio	Peak Load (lb/ft^2)	Load Duration (sec)	Peak Footing Acceleration (g)	Peak Displacement (in.)	Time to Peak Displacement (sec)	Initial Rate of Displacement (in./sec)	Excess Pore Pressure[2] at 8-1/2-Foot Depth (psi)	Pore Pressure Wave Arrival Time[3] (sec)
4-65[1]	100	0.48	10,619	0.993	44.6	0.352	0.010	75.90	0.344	0.015
5-65	100	0.48	19,875	1.165	57.0	0.468	0.008	105.36	0.458	0.013
6-65	100	0.46	23,688	0.830	73.5	0.559	0.009	122.04	0.635	0.012
7-65	100	0.45	29,863	0.947	137.0	1.230	0.008	254.53	0.942	0.012
8-65	100	0.41	38,976	0.728	142.0	0.862	0.007	197.31	0.982	0.012
9-65	drained	0.40	13,064	1.033	35.7	0.332	0.008	117.89	0.229	0.013
10-65	drained	0.45	24,074	1.018	67.0	0.586	0.009	186.79	0.520	0.012
11-65	drained	0.50	35,769	1.020	92.7	0.606	0.008	135.30	0.809	0.011
12-65	drained	0.41	31,918	0.700	72.6	0.580	0.008	194.64	0.641	0.012
13-65	100	0.50	11,052	1.118	43.0	0.426	0.010	68.45	0.233	0.015
14-65	drained	0.54	10,266	1.058	40.4	0.428	0 010	66.40	0.231	0.014
15-65	100	0.54	22,556	1.167	64.9	0.910	0.012	123.64	0.462	0.013
16-65	100	0.50	35,332	1.277	114.7	1.182	0.010	285.69	0.816	0.012
17-65	drained	0.51	23,385	1.147	39.7	0.794	0.012	108.66	0.350	0.013
18-65	drained	0.54	23,284	1.019	72.1	0.655	0 010	112.93	0.286	0.013
19-65	100	0.53	36,573	1.031	90.2	1.435	0.010	217.17	0.446	0.012

1/ Tests 1, 2, and 3 were auxiliary tests and not a part of this series.
2/ That is, greater than the ambient static equilibrium condition.
3/ Zero time was taken as the arrival time of the dynamic load on the top of the footing as indicated by an accelerometer.

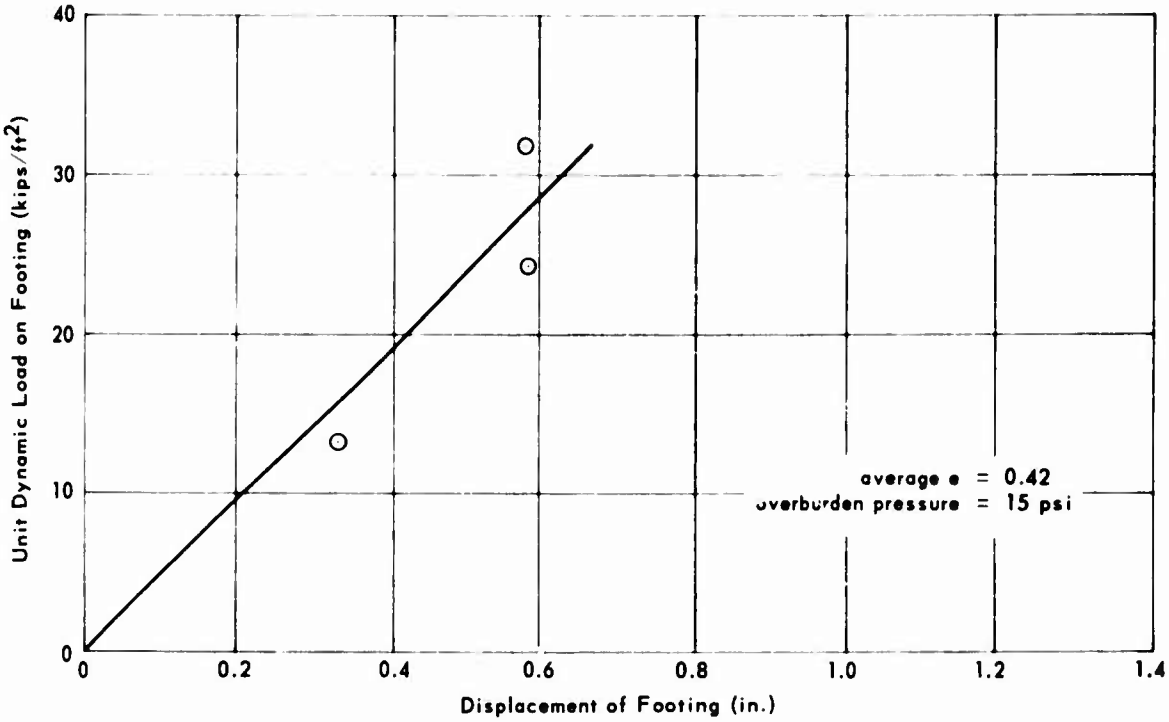

Figure 10. Dynamic load versus displacement of a 1-foot by 6-foot footing in drained sand; data from tests 9, 10, and 12 shown as line A in Figure 16.

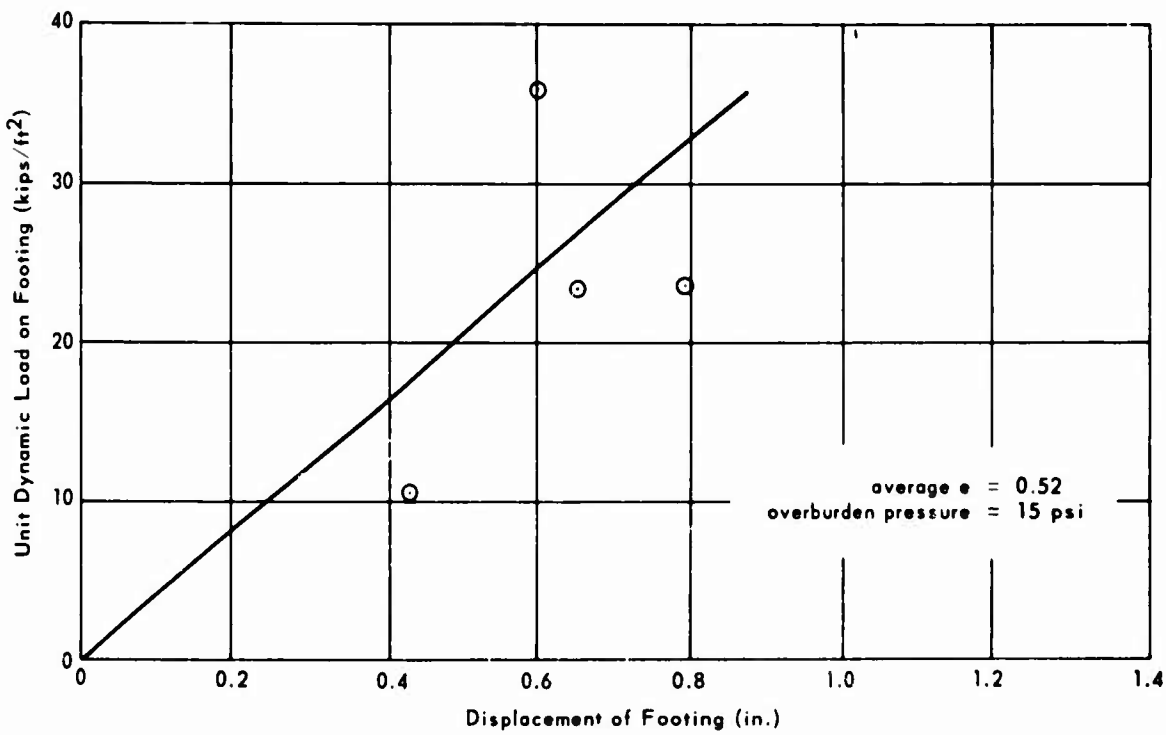

Figure 11. Dynamic load versus displacement of a 1-foot by 6-foot footing in drained sand; data from tests 11, 14, 17, and 18 shown as line B in Figure 16.

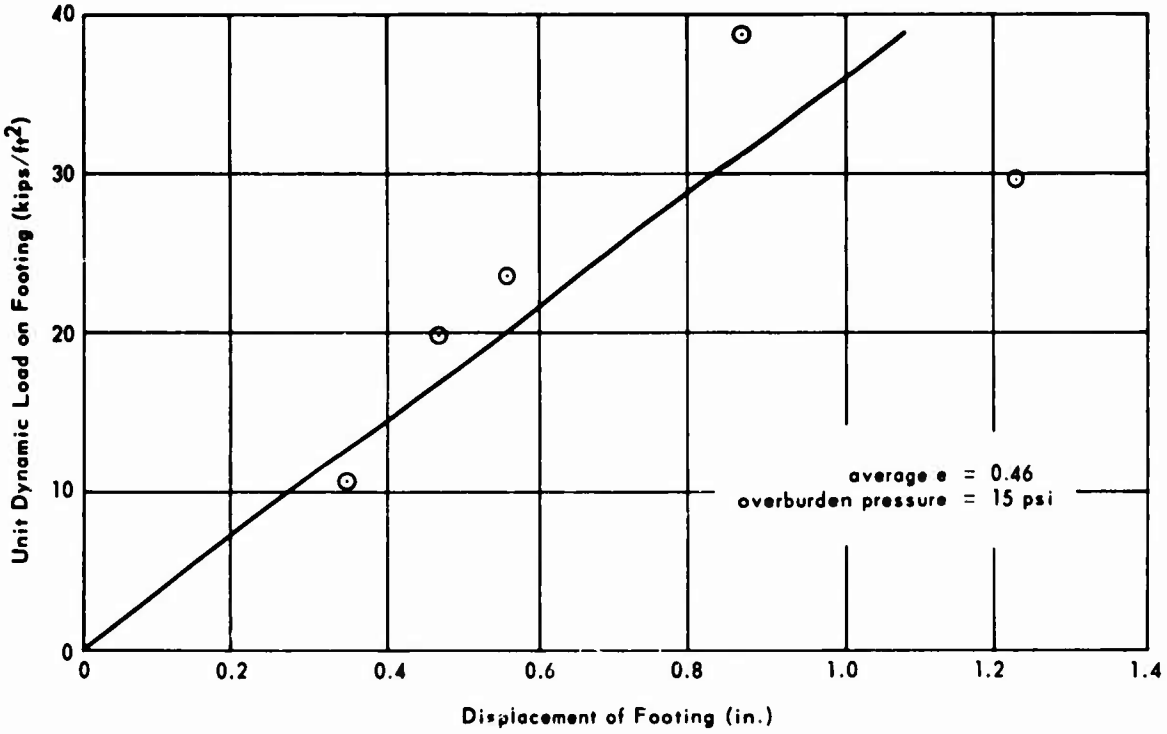

Figure 12. Dynamic load versus displacement of a 1-foot by 6-foot footing in saturated sand; data from tests 4, 5, 6, 7, and 8 shown as line C in Figure 16.

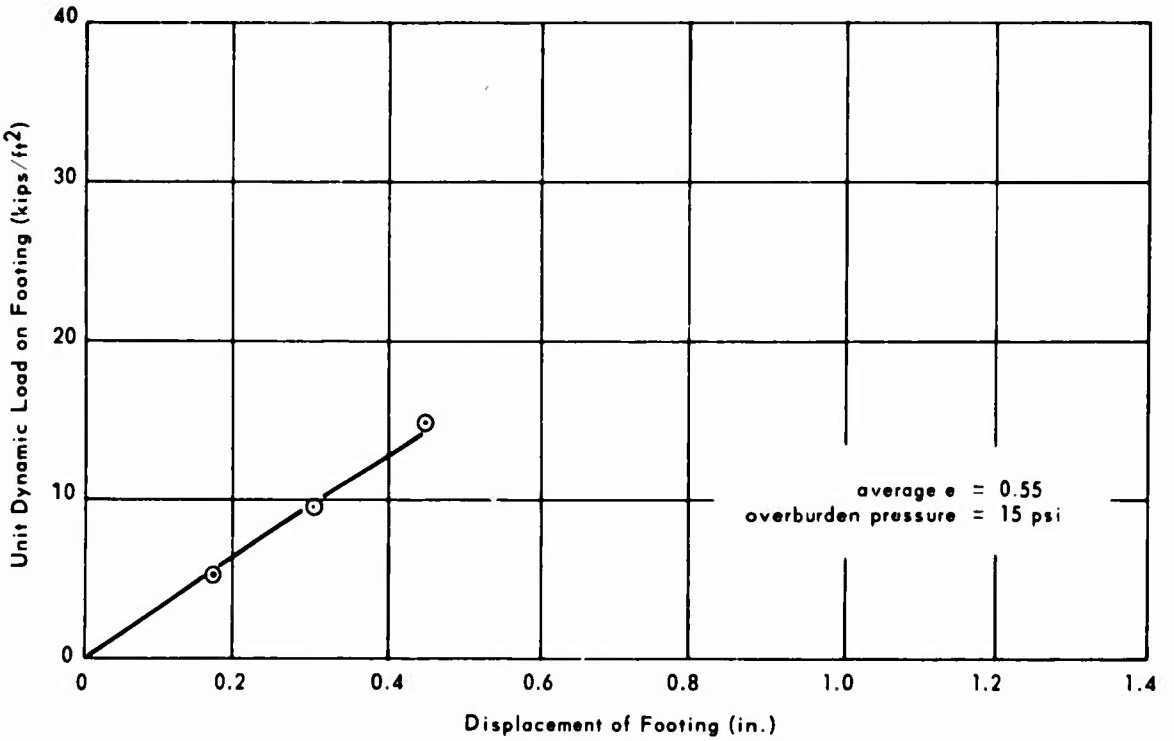

Figure 13. Dynamic load versus displacement of a 1-foot by 6-foot footing in dry sand; data from Reference 3 shown as line D in Figure 16.

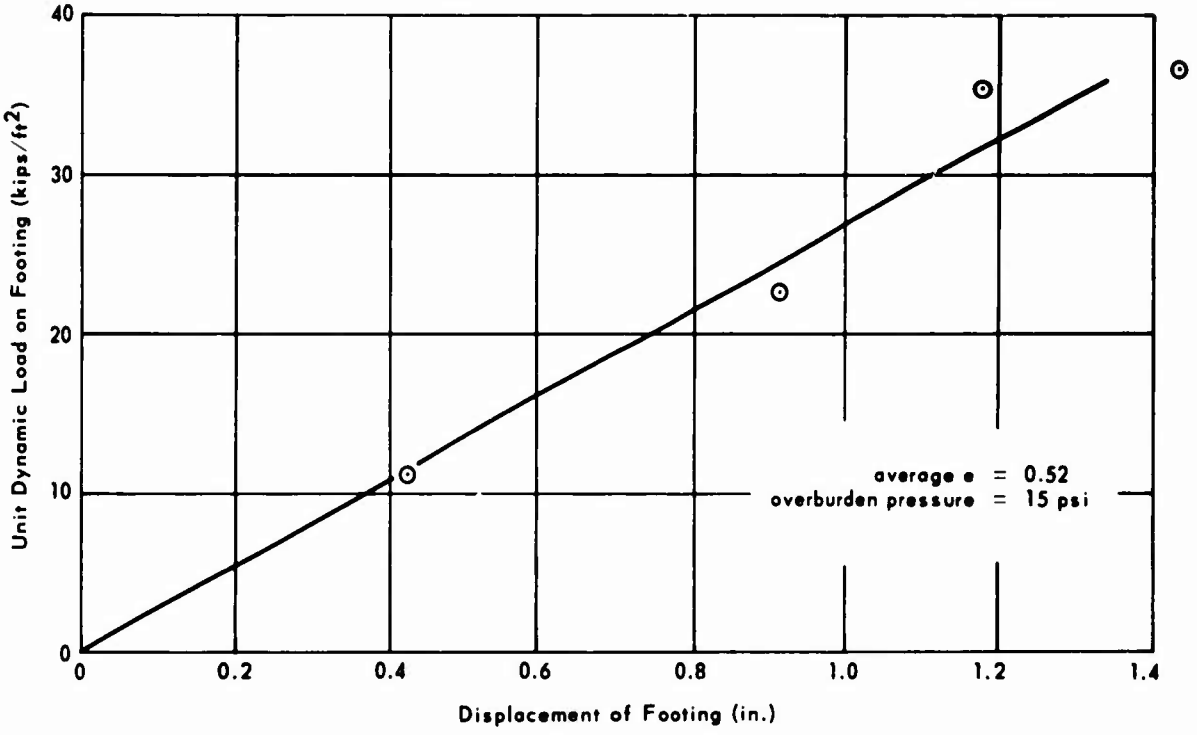

Figure 14. Dynamic load versus displacement of a 1-foot by 6-foot footing in saturated sand; data from tests 13, 15, 16, and 19 shown as line E in Figure 16.

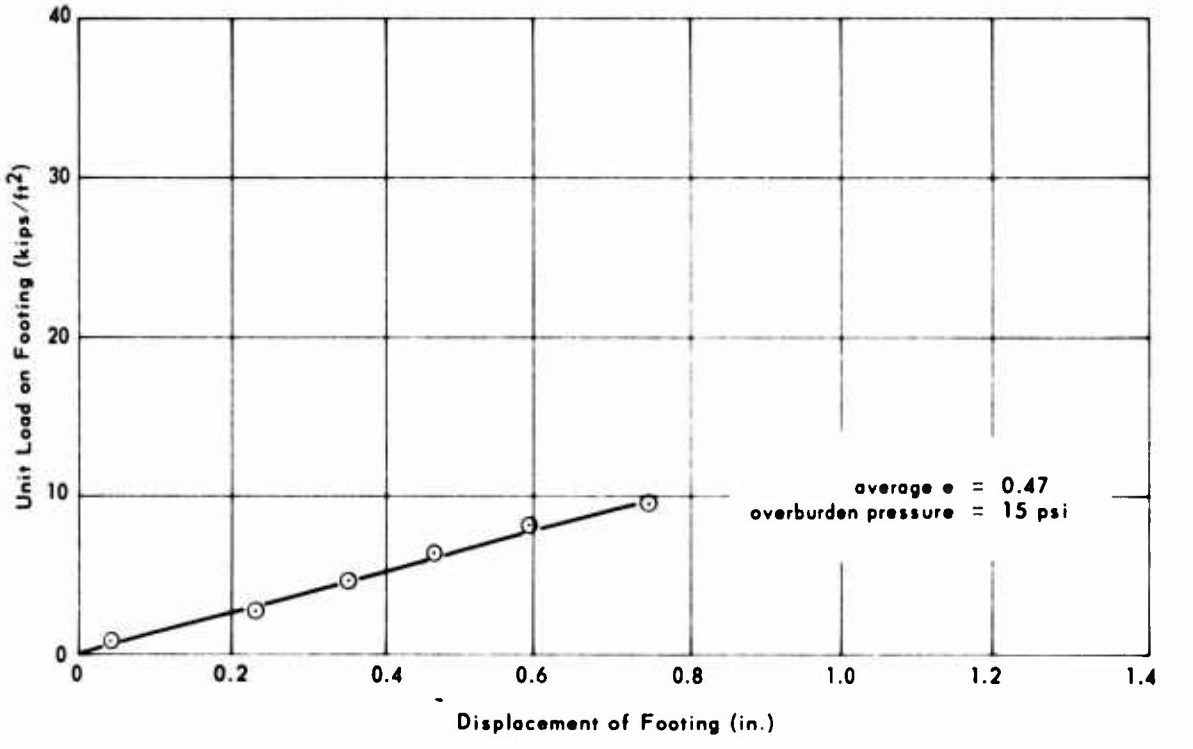

Figure 15. Static load versus displacement of a 1-foot by 6-foot footing in saturated sand; data from test 1S-65 shown as line F in Figure 16.

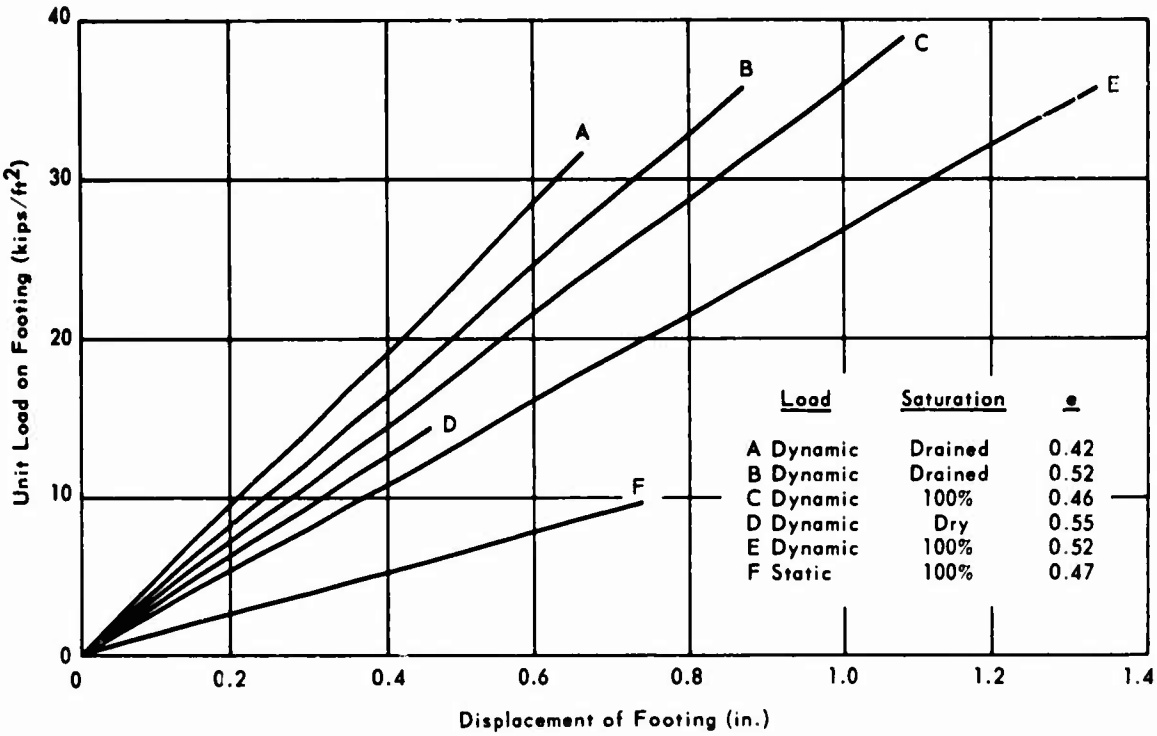

Figure 16. Composite graph of load-displacement relationships of a 1-foot by 6-foot footing loaded statically and dynamically in saturated, drained, and dry sand at various void ratios and under 15-psi overburden. Data for individual lines shown in Figures 10 through 15.

Table 3. Load-Displacement Data for 12-Inch-Wide by 18-Inch-Deep by 6-Foot-Long Footing Loaded Statically in Saturated Sand

(15-psi overburden at one side of footing; initial void ratio = 0.47)

Load on Footing (lb/ft^2)	Footing Displacement (in.)
0	0
930	0.048
2,753	0.232
4,650	0.350
6,285	0.465
8,099	0.599
9,457	0.743
8,092	1.287
0	1.010

By definition, the void ratio (e) of a soil is the ratio of the volume of voids to the volume of solid matter comprising the soil skeleton. The definition does not differentiate between voids which are occupied by gas or liquid or by combinations of gas and liquid. There is, for a given soil, some void ratio at which the soil neither expands nor contracts when sheared. This condition is termed the critical void ratio, e_{cr}. At void ratios higher than e_{cr}, the soil contracts along shear planes. At void ratios lower than e_{cr}, the soil expands along shear planes. A saturated soil is one having all pore spaces filled with liquid. When a saturated soil is loaded to failure at other than e_{cr}, water must migrate toward or away from shear surfaces according to whether the soil initially was below or above e_{cr}. If the rate of load application and the magnitude of soil permeability are such that pore water conditions on the shear surface do not remain in equilibrium as the load is applied, the shear strength will be affected. Under these conditions, and at an initial void ratio higher than e_{cr}, there will develop on the shear surface an excess pore pressure. This excess pore pressure causes a decrease of intergranular stress and a consequent reduction of shear strength. Conversely, an initial void ratio lower than e_{cr} will result in a decreasing pore pressure on the shear surface, which may ultimately produce a condition of cavitation in the pore water. This produces an increase in intergranular stress in the soil skeleton along the shear surface with a consequent increase in shear strength. These critical void ratio effects have been experimentally examined by other researchers in small-sized shear tests.[8]

The footing tests reported here were examined to determine if void ratio conditions (both above and below e_{cr}) would influence the load-displacement behavior of a large footing loaded dynamically in saturated soil. The critical void ratio effect should not operate in dry soil, in soil at less than 100% saturation, nor in soil which is loaded statically (i.e., loaded slowly enough to permit pore pressures to remain in equilibrium). To effect the desired comparisons, one test of this series was made under static loading conditions. Several tests were made in saturated soil, and several were made with the soil in a drained condition (i.e., less than 100% saturation). The data used to produce Figure 13 are from dynamic tests in dry sand that were made under a test series reported earlier.[3]

As a preamble to consideration of the test results, it should be noted that the ratio of footing load to footing displacement is an index of soil bearing properties. It is often termed "k value" or soil modulus of reaction and is expressed in units of unit load per unit displacement. If the critical void ratio factor described above is not operative (e.g., when loading-rate versus permeability permits equilibrium to prevail, or when saturation is less than 100%), the k value is partially and inversely a function of void ratio. This is because soil bearing strength is related to shearing strength which is inversely related to void ratio.

The purpose of the following discussion is to examine the effects upon k value of the interrelationships among void ratio, degree of saturation, and type of load (i.e., static or dynamic). For the analysis, the various tests have been categorized

on the basis of type of load, and condition of saturation; and within those two categories, upon the basis of high or low void ratio. High void ratios are here defined as those of 0.50 or higher. Low void ratios are less than 0.50. To make the discussion concise, the test groups will be referred to as "A," "B," "C," etc. Soil and test conditions are shown in the composite graph of Figure 16, in the captions of Figures 10 – 15 from which Figure 16 was constructed, and in Table 4.

Table 4. Soil and Test Conditions Illustrated in Figure 16

Test Group	Test Numbers in Group	Type of Load	Moisture Condition	Average Void Ratio, e, of Group	Load-displacement Ratio, k, (psi/in.)
A	9, 10, 12	dynamic	drained	0.42	332
B	11, 14, 17, 18	dynamic	drained	0.52	286
C	4, 5, 6, 7, 8	dynamic	saturated	0.46	250
D	from Ref. 3	dynamic	dry	0.55	219
E	13, 15, 16, 19	dynamic	saturated	0.52	186
F	—	static	saturated	0.47	91

1. A versus B

In this comparison, the critical void ratio effect should not be operative. The relative magnitudes of the average void ratios of the two groups would tend to make the k value of group A larger than that of group B, as the experimental results show it to be.

2. A versus C

Group A is drained, so the critical void ratio effect should not be operative in that group. Group C is saturated and susceptible to the critical void ratio effect. The void ratios of the two groups are quite similar, and without the e_{cr} effect the k values would be similar, with that of group C being slightly the smaller. If e_{cr} for this soil is less than the void ratio of group C (0.46), then the difference in k values of the two groups is probably larger than it would have been without the e_{cr} effect. Conversely, if e_{cr} is larger than 0.46, the k value of group C probably would be larger than that of group A. Thus, the relative positions of A and C on the graph suggest that e_{cr} is less than 0.46.

3. A versus D

Since group A is drained and group D is dry, the critical void ratio effect should not be operative; and the higher void ratio of group D should produce a smaller k value for group D than that exhibited by group A. The graph of Figure 16 confirms this.

4. A versus E

If the hypothesis of item 2 above is correct (i.e., e=0.46 is larger than e_{cr}), then e = 0.52 of group E also must be larger than e_{cr}. Group E is dynamically loaded and saturated, and therefore subject to the e_{cr} effect. In this instance, that effect would be a reduction in the k value of group E. Group A is not subject to the e_{cr} effect. The magnitude of the difference in k value between groups A and E probably is greater because of the e_{cr} effect on group E than it might have been if caused only by the difference in e between the two groups.

5. A versus F

As hypothesized earlier, the e_{cr} effect should not be operative in a static condition such as group F, nor in a drained dynamic test such as group A. Even though e of group A is only slightly lower than that of group F, group A has a considerably higher k value than group F. This parallels earlier experience[1,2] with dynamic-versus-static bearing tests in dry sand where the e_{cr} effect is definitely not a factor.

6. B versus C

If e_{cr} effect were not operative, the k value of group C would be larger than that of group B, based upon the relative magnitudes of their void ratios. That the k value of group B is larger than that of group C reaffirms the operation of e_{cr} effect on dynamically loaded, saturated soil, and further confirms that e = 0.46 is larger than e_{cr}. In this comparison, the e_{cr} effect is more influential in establishing the relative magnitudes of k than are the relative magnitudes of e of the two groups.

7. B versus D

In this comparison, the e_{cr} effect should not be operative. The relative values of the void ratios of the two groups should cause the k value of group B to be larger than that of group D, which it proves to be.

8. B versus E

This comparison offers an excellent opportunity to observe the critical void ratio effect, because the void ratios of the two groups are identical. Group B, being drained, should not be affected. Group E, being saturated, should be affected. As may be seen in Figure 16, the k value of group E is considerably smaller than that of group B. This fact most probably is attributable to the e_{cr} effect, and strongly supports the contention of item 4 above that e = 0.52 is larger than e_{cr}.

9. B versus F

In this comparison, the e_{cr} effect is not operative. Even though the e of dynamically loaded group B is considerably higher than that of statically loaded group F, the k value of group B is larger than that of group F. This once again indicates the strong tendency for dynamic k to be higher than static k even when relative void ratios are such as to encourage the opposite.

10. C versus D

According to the hypothesis being examined here, the e_{cr} effect should be operating on group C. This effect (when e is larger than e_{cr}) tends to cause a reduction of k. However, the difference in void ratios (0.46 versus 0.55) is great enough to be more influential than the e_{cr} effect in establishing the relative magnitude of k between the saturated condition of group C and the dry condition of group D. The difference in k values would be even greater if the e_{cr} effect were not acting upon group C.

11. C versus E

In this case, both groups represent dynamic tests under saturated conditions. If the e = 0.46 of group C is larger than e_{cr} (as suggested earlier), then e = 0.52 (group E) must also be larger than e_{cr}. Therefore, it would be impossible to assess the relative influence of the e_{cr} factor on the two groups of tests. At least, the relative magnitudes of k value are correct for the relative magnitudes of void ratio.

12. C versus F

In this comparison, the void ratios of the two groups are essentially equal. Both test groups are saturated. If, as presumed, the e_{cr} effect is operating on the dynamically loaded group C, then the k value of group C is smaller than it might otherwise be. However, the k value of group C was not reduced enough to negate the earlier observation[1,2] that dynamic k value tends to be larger than the static value.

13. D versus E

In this comparison, the void ratios of the two groups are similar, but the slightly lower void ratio of group E should make the k value of group E larger than that of group D. Figure 16 reveals that this is not the case. Apparently the e_{cr} effect (which can operate on group E and not on group D) predominates in establishing the relatively smaller k value of group E.

14. D versus F

The e_{cr} effect should not apply in this comparison, since the dynamic case (group D) is dry and the saturated case (group E) is statically loaded. Therefore, this comparison merely supports the earlier conclusion[1,2] that dynamic k values tend to be larger than static k values. This tendency is shown here to prevail even though the relative e values of the two test groups would tend to produce the opposite relative magnitudes of k value.

15. E versus F

In this comparison, three factors are interacting. They are: (1) the tendency for the relatively lower e of group F to cause the k value of group F to be relatively larger than that of group D; (2) the tendency for the k value of group E to be reduced by the e_{cr} effect; and (3) the tendency for dynamic k value to be larger than static k value. The first two of these factors tend to make the k value of group F larger than that of group E. The third and apparently most influential of the three acts to establish the relative k values of groups E and F as they are shown in Figure 16.

Despite the fact that void ratios lower than critical were not achieved in these experiments, the results shown in Figures 10 through 16 are useful. If the critical void ratio factor does operate at void ratios lower than critical, the effect would be to make the displacements shown in the figures conservative. That is, the footing displacement for a specified load in saturated sand would be less than shown. This fact should be taken into consideration if Figures 10 through 16 are used for the preliminary design of footings on saturated sands at void ratios lower than those shown.

CONCLUSIONS

The conclusions listed below are based upon the results of tests reported here and upon the results of earlier test series.[1, 2, 3] These conclusions apply to sand loaded statically and dynamically in bearing.

1. The magnitude of the modulus of subgrade reaction, k, is inversely related to the magnitude of the initial void ratio, e. (Initial void ratio effect.)

2. Sand loaded dynamically has a larger k value than sand loaded statically. (Dynamic loading effect.)

3. Dynamically loaded sand at a void ratio larger than the critical void ratio has a smaller k value when saturated than when less than saturated. (Critical void ratio effect.)

4. The dynamic loading effect exerts a stronger influence upon the magnitude of the k value than does the relative magnitude of the initial void ratio.

5. The dynamic loading effect exerts a stronger influence upon the magnitude of the k value than does the critical void ratio effect.

6. The critical void ratio effect should not operate in sand loaded statically, whether it is saturated or not.

7. The critical void ratio effect should not operate in sand loaded dynamically at less than 100% saturation.

FUTURE PLANS

Stress wave propagation in the pore fluids of soils loaded at a free boundary has not been well defined. These pore fluid stresses may have important effects upon buried structures. Specifically, they may have a direct influence upon the void ratio effects discussed in this report and thus upon the behavior of dynamically loaded buried footings. A theoretical analysis has been completed.[9] Preparations are in progress for experiments to verify or modify the theories. Some of the significant variables to be investigated are soil particle size, particle size distribution, moisture content and degree of saturation, soil relative density, soil compressibility, range and duration of overpressure, and relationship to permeability. Soil types will encompass cohesive and noncohesive materials. Dynamic gas pressures will be applied to free water surfaces standing on saturated soils, to saturated soils with no free water on the upper surface, and to the upper surfaces of soils having a water table below the surface. The principal load variables will be magnitude and duration. Phenomena of interest in the interiors of the soil specimens will include magnitudes of changes in intergranular stress, magnitudes of excess pore pressure, and the time phase relationship between the two.

In another area of investigation, both theoretical and experimental studies are planned to investigate the effects of the magnitude and of the arrival time of dynamic surcharges (produced by air blast loadings) on the load-displacement behavior of buried footings. This work will involve both noncohesive and cohesive soils at various degrees of saturation.

Other experiments are planned to evaluate the effect of footing width on the load-displacement behavior of dynamically loaded strip footings.

ACKNOWLEDGMENTS

Personnel of the Trades Department are commended for excellent performance of a difficult job. M. C. Chapman of the Soils and Pavements Division directed the physical performance of the experiments and was assisted by R. Lorenzana of the Soils and Pavements Division in reduction of the test data to a usable format. J. R. Allgood of the Structures Division provided an excellent critical review of the manuscript.

REFERENCES

1. U. S. Naval Civil Engineering Laboratory. Technical Report R-277: Static and dynamic plate-bearing tests on dry sand without overburden, by C. R. White. Port Hueneme, Calif., Jan. 1964.

2. ———. Technical Report R-338: Static and dynamic plate-bearing tests on dry sand with overburden, by C. R. White. Port Hueneme, Calif., Sept. 1964.

3. ———. Technical Report R-387: Dynamically loaded strip footing buried in dry sand, by C. R. White. Port Hueneme, Calif., Aug. 1965.

4. U. S. Army Engineer Waterways Experiment Station. Technical Report no. 3-599-4: Dynamic bearing capacity of soils. Investigation of a dimensionless load-displacement relation for footings on clay, by P. F. Hadala. Vicksburg, Miss., June 1965. (AD 467081)

5. U. S. Defense Atomic Support Agency. Report WT-1422: Operation PLUMBBOB, Nevada Test Site, May-October 1957: Evaluation of buried corrugated-steel arch structures and associated components, by G. H. Albright et al. Albuquerque, N. M., Feb. 1961. (AD 615737)

6. W. A. Shaw and J. R. Algood. "An atomic blast simulator," Society for Experimental Stress Analysis, Proceedings, vol. 17, no. 1, 1959, pp. 127-134.

7. U. S. Naval Civil Engineering Laboratory. Technical Note N-585: Static and dynamic shear strength of dry sand, by R. L. Lytton and C. R. White. Port Hueneme, Calif., Apr. 1964.

8. H. B. Seed and R. Lundgren. "Investigation of the effect of transient loading on the strength and deformation characteristics of saturated sands," American Society for Testing Materials, Proceedings, vol. 54, 1954, pp. 1288-1306.

9. U. S. Naval Civil Engineering Laboratory. Technical Note N-776: Theoretical analysis of dynamic pressure propagation in the pore fluids of soils, by J. W. Fead. Port Hueneme, Calif., Oct. 1965.

BLANK PAGE

Unclassified

Security Classification

DOCUMENT CONTROL DATA - R & D

Security classification of title, body of abstract and indexing annotation must be entered when the overall report is classified

1 ORIGINATING ACTIVITY (Corporate author) Naval Civil Engineering Laboratory Port Hueneme, California	2a REPORT SECURITY CLASSIFICATION Unclassified 2b GROUP

3 REPORT TITLE

Static and Dynamic Bearing Tests on a Strip Footing in Saturated Sand

4 DESCRIPTIVE NOTES (Type of report and inclusive dates)

Not final; January 1965 to May 1966

5 AUTHOR(S) (First name, middle initial, last name)

Charles R. White

6 REPORT DATE	7a TOTAL NO OF PAGES	7b NO OF REFS
June 1967	25	9

8a CONTRACT OR GRANT NO DASA-13.018 b PROJECT NO Y-F008-08-03-402 c d	9a ORIGINATOR'S REPORT NUMBER(S) TR-536 9b OTHER REPORT NO(S) (Any other numbers that may be assigned this report)

10 DISTRIBUTION STATEMENT

Distribution of this report is unlimited. Copies available at the Clearinghouse for Federal Scientific & Technical Information (CFSTI), Sills Building, 5285 Port Royal Road, Springfield, Va. 22151 - Price $1.00.

11 SUPPLEMENTARY NOTES	12 SPONSORING MILITARY ACTIVITY
	Defense Atomic Support Agency and Naval Facilities Engineering Command

13 ABSTRACT

This report describes the static and dynamic loading of a 12-inch-wide by 18-inch-deep by 6-foot-long rigid footing, representing the strip footing of a subsurface shelter. Boundary conditions simulated those of a torsionally restrained footing of a flexible arch structure with simulated overburden of 20 feet at one side of the footing. Saturated and partially saturated sand was the test soil. Several soil void ratios were employed, and the effect on the relationship between load and displacement of the footing caused by soil saturation at void ratios higher than the critical void ratio was demonstrated.

DD FORM 1 NOV 65 1473 (PAGE 1)

S/N 0101-807-680

Unclassified

Security Classification

14 KEY WORDS	LINK A		LINK B		LINK C	
	ROLE	WT	ROLE	WT	ROLE	WT
Strip footing						
Bearing tests						
Static tests						
Dynamic tests						
Saturated sand						
Subsurface shelter						
Flexible arch						
Void ratios						
Critical void ratio						
Soil bearing capacity						
Simulated overburden						
Soil dynamics						
Blast overpressure						
Operation PLUMBBOB						